ELSEVIER

Variable temperature system using vortex tube cooling and fiber optic temperature measurement for low temperature magic angle spinning NMR

Rachel W. Martin and Kurt W. Zilm*

Department of Chemistry, Yale University, P.O. Box 208107, New Haven, CT 06520-8107, USA

Abstract

We describe the construction and operation of a variable temperature (VT) system for a high field fast magic angle spinning (MAS) probe. The probe is used in NMR investigations of biological macromolecules, where stable setting and continuous measurement of the temperature over periods of several days are required in order to prevent sample overheating and degradation. The VT system described is used at and below room temperature. A vortex tube is used to provide cooling in the temperature range of −20 to 20 °C, while a liquid nitrogen-cooled heat exchanger is used below −20 °C. Using this arrangement, the lowest temperature that is practically achievable is −140 °C. Measurement of the air temperature near the spinning rotor is accomplished using a fiber optic thermometer that utilizes the temperature dependence of the absorption edge of GaAs. The absorption edge of GaAs also has a magnetic field dependence that we have measured and corrected for. This dependence was calibrated at several field strengths using the well-known temperature dependence of the ^{1}H chemical shift difference of the protons in methanol.
© 2004 Elsevier Inc. All rights reserved.

Keywords: MAS NMR; Sample heating; Temperature measurement; Temperature sensor magnetic field dependence; Variable temperature NMR; Vortex tube

1. Introduction

Variable temperature (VT) capability is a necessary component of a fast MAS probe to be used in investigations of biological macromolecules. These samples are often temperature sensitive, with the dissolution of crystals, loss of activity, or disruption in structure occurring even at moderate temperatures. To perform structural studies on this type of sample at high magnetic field, reproducible measurement, and control of temperature over a period of several days is needed.

Fast magic angle spinning, which becomes increasingly important at higher field, generates heating via friction between the outside of the rotor and the bearing gas. This effect has been most thoroughly documented using the temperature dependence of the ^{207}Pb chemical shift of lead nitrate [1–3]. Especially at high spinning

speeds, the difference between the ambient temperature of the air surrounding the rotor and the temperature measured inside the sample can be very large [4]. Using smaller rotors will ameliorate this effect, since frictional heating depends on the peripheral velocity, which scales with the spinning speed and the radius of the rotor [5]. However, heating does occur even in smaller rotors and at moderate spinning speeds.

The majority of biochemical samples are also electrically lossy, and interact with the probe electronics. This in turn leads to sample heating even without sample spinning. Hydrated samples of high ionic strength are conductive, and many macromolecular systems, such as proteins, are inherently lossy dielectrics. Interaction of the sample with the radio frequency (RF) electric field inside the sample coil, either because of conductivity or dielectric loss, provides a mechanism for generating heat within the sample. Sample loading of RF electronics is a well-known problem in solution NMR [6], magnetic resonance imaging [7], and in the

---

* Corresponding author. Fax: 1-203-432-6144.
E-mail address: kurt.zilm@yale.edu (K.W. Zilm).

operation of cryoprobes [8]. The loading of the probe Q by the sample also leads to a decrease in probe efficiency. This is usually most pronounced for the ^{1}H channel, and can result in a shift of the Hartmann–Hahn condition for optimal cross-polarization. Since the effective resistance generated by the sample loading can depend upon the sample's temperature, the probe Q can also appear temperature dependent as the sample heats during a long RF pulse. This can lead to probe tuning instability, as well as duty factor and sample dependent RF field matching conditions, and is not conducive to obtaining quality data in many experimental situations.

Approaches to ameliorating RF induced sample heating in liquids NMR have included simply reducing the sample volume [9] or using higher thermal conductivity sample tubes to maximize heat exchange between the sample and the stream of cooling gas [10]. A more widely adopted approach is to use a low-inductance, shielded coil design to reduce electric fields in the sample [11]. None of these options are easily applicable to MAS NMR of biological samples. Sample rotors for fast MAS must be made from high tensile strength materials such zirconia or other ceramics which all have poor thermal conductivity. Specialized decoupler coil designs are difficult to adapt for use in this application because of the constraints of the MAS sample geometry and the single coil design chosen for the triple resonance probe described. Efficient removal of heat by sample cooling is then a necessity. Since cooling of the sample can usually render biological solids NMR samples much less lossy, this is often a requirement to obtain stable performance in many experiments.

The VT system described here introduces cold gas through the bottom of the probe via a flexible connection. This allows samples to be conveniently changed at low temperature, enabling studies of samples that must be constantly kept cold. In many instances temperatures no lower than $-20\,^\circ$C are required, making it possible to use a Ranque–Hilsch vortex tube [12,13] to supply the cooling air. This device produces a cold stream of gas using only a high-pressure room temperature air supply. Using the vortex tube for cooling is therefore no more difficult that supplying room temperature purge air. This method of cooling is used essentially all the time in our laboratory unless lower temperatures are desired. When lower temperatures are required a commercial liquid nitrogen cooled heat exchanger is used.

Successful variable temperature operation for MAS of biological samples also requires continuous monitoring of the sample temperature. Although the lead nitrate chemical shift thermometer for MAS NMR is reliable and well-characterized, it is not suitable for use as an internal standard in this application. The triple resonance probe used in our laboratory to study proteins and other macromolecular systems is optimized for ^{1}H/^{13}C/^{15}N operation and is not broad-banded [14]. As

such it has a fairly small frequency range and cannot tune to the frequency required to detect ^{207}Pb. A chemically inert NMR thermometer that could be included in each sample as an internal standard and using a nucleus with a resonant frequency close to that of ^{13}C would be very useful in this type of application. Unfortunately such a temperature standard for solid state NMR has not been developed. For the time being it is safer to use more moderate spinning speeds in conjunction with cooling of the air stream in order to ensure that samples are not damaged by overheating.

Because of this limitation it is necessary to use an external temperature sensor located as close as possible to the rotating sample to detect any temperature rise in the air surrounding the rotor due to friction. Typically instruments such as thermocouples or diodes have been used in this type of application, however these devices require an electrical connection between the transducer and the external device which provides for readout of the temperature. These electrical connections can interfere with the RF electronics of the probe, an especially significant problem at 800 MHz. To prevent coupling to the RF electronics these devices must be located far away from the primary RF coil, which limits their utility since the temperature being measured is then far away from the sample. Even when located far enough away to not measurably affect the probe efficiency, these leads usually introduce extra noise into the probe unless special precautions are taken to filter it out, as the electrical leads can act as an antenna bringing extraneous RF signals into the probe. Furthermore, when high power RF decoupling is used, RF power can inadvertently be transmitted down the leads of a thermocouple or similar device. This can be sufficient to overload and in some instances even damage the detector electronics.

Fiber optic temperature sensors avoid these problems by using a non-conductive optical fiber to transmit the temperature information from the sample region to the temperature conversion electronics. Having no conductive leads, such sensors can be placed arbitrarily close to the sample, limited only by the logistics of spinning and by field homogeneity requirements. The particular type of fiber optic thermometer used here employs a small GaAs crystal as the sensor on the end of a standard silica optical fiber. To date we have not observed any unusual change in field homogeneity that could be attributed to the sensor. The sensor functions over a range from liquid nitrogen temperature to above room temperature, which corresponds well to the desired operating temperatures for biological macromolecules. The only precaution one must take in using this type of device is to account for the magnetic field dependence of the sensor response. In this work we find the required correction to be a simple magnetic field dependent constant offset in the apparent temperature.

2. Characterization of sample heating and sample Q-loading

Although using small rotors reduces frictional heating effects, sample cooling is still required at even moderate spinning speeds. Fig. 1 illustrates the difference in temperature between the air surrounding the rotor and the actual sample for a 3.2 mm rotor. These temperatures were first measured using the ^{207}Pb chemical shift of lead nitrate [1–3] inside the rotor, and again outside the magnet by placing a thermocouple as close as possible to the spinning sample. In a 3.2 mm rotor with no VT flow the sample temperature can be significantly higher than the surrounding air temperature. This temperature differential is negligible at spin rates less than 10 kHz, is only about 5 °C at 15 kHz spinning, but rapidly increases to as much as 28 °C at 25 kHz spinning. Passing cooling air over the sample alleviates the problem considerably. In this particular experiment the VT stream was cooled to ∼4 °C. This brings the temperature of the sample with 25 kHz MAS down to 25 °C rather than the 60 °C it would be with no cooling. Even with VT operation a delta remains between the surrounding air temperature and the sample temperature. The additional airflow and cooling reduces this delta at 25 kHz to 17 °C, whereas a delta of 28 °C is measured without VT. For biological studies it is important to recognize that the temperature can increase rapidly with spin rate even with small diameter rotors, and that the temperature of the air surrounding the spinning sample may be significantly lower than the sample temperature even with active sample cooling. Failure to use cooling gas at all times, even when just initially spinning up a sample, can make the difference between having a denatured sample and an intact one.

Coupling of the probe electronics to a typical protein sample can be characterized by following the probe tuning or Q-loading as a function of VT gas flow temperature. Freezing the sample in principle should restrict the thermal motions of any ionic components that produce conductivity losses, and freeze out the molecular motions responsible for dielectric loss. Because of the colligative properties of the salt and the organic precipitating agents, temperatures well below 0 °C may be needed to freeze this type of sample. These effects can be qualitatively assessed by following the position of the probe ^{1}H tuning resonance as a function of temperature. In our measurements this has been monitored using a Hameg spectrum analyzer with tracking generator and a reflection bridge.

Since the bulk of the coil volume is filled by the high dielectric zirconia rotor, a large shift the order of 4 MHz is always observed when a rotor is placed in the probe. The absolute tuning shift measured is somewhat dependent on the actual rotor used, and is difficult to measure accurately. The principal sources of error are the minute to minute random fluctuations on the order of ±0.25 MHz in the Hameg frequency standard, as well as slower systematic drift in this standard. Nevertheless, the trends observed as a function of temperature are reproducible. For an empty rotor, or one filled with a relatively lossless sample such as adamantane, the tuning position remains constant to within ±0.25 MHz as a function of temperature from room temperature down to −140 °C. A typical lossy protein sample will shift the probe tuning by an additional 1.0–1.5 MHz at room temperature. This additional shift for hydrated protein samples is always seen to be a function of temperature, and typically disappears as the temperature is dropped. For a typical sample of hydrated ubiquitin nanocrystals prepared using 200 mM cadmium acetate and 25% weight by volume PEG 2000, the tuning shift reproducibly drops by ∼1 MHz from −30 to −50 °C. This temperature window is also coincidentally where this sample appears to go through a glass transition [15]. While these measurements do not distinguish among the possible molecular mechanisms by which the sample can couple to the electric field in the sample coil, they do highlight the fact that these losses are temperature dependent, and can be suppressed by lowering the sample temperature. As a low power single frequency temperature dependent RF loss measurement, this approach is a convenient one for determining how low a sample need be cooled to minimize Q-loading of the probe, and thus any associated heating by absorption of RF power.
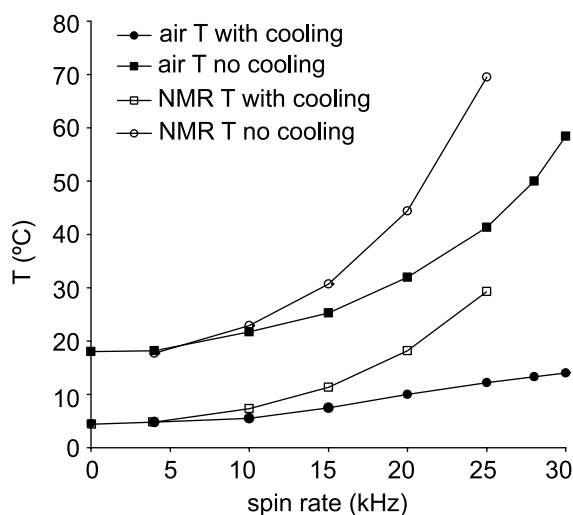

Fig. 1. Temperature plotted as a function of spinning speed, with and without cooling of the air surrounding the sample. A Chemagnetics style 3.2 mm stator was used which has baffles separating the airflow in the VT compartment from the air bearing flow. The "air" temperature with cooling (●) and without cooling (■) was measured by a thermocouple near the sample. The "NMR" temperature with cooling (□) and without cooling (○) was measured using the ^{207}Pb chemical shift of lead nitrate.

3. Low temperature VT apparatus

Pre-cooled VT nitrogen enters at the bottom of the probe and travels to just below the stator via a glass dewar located slightly forward of the center of the probe body. This dewar is constructed from glass tubing (9 mm OD outer tubing, 4 mm OD inner tubing) and is 25.25 in. from the point where it meets the stator to the point where it makes a right angle bend at the bottom of the probe. The dewar was initially evacuated to 8×10^{-7} Torr while being heated to 150 °C before flame sealing. Connection between the dewar and the stator is made with flexible Teflon tubing. The Teflon tubing is affixed to the glass dewar using Teflon heat shrink tubing to ensure that the VT stream is fully directed into the stator. A small hole in the plastic tubing admits the fiber optic temperature sensor, permitting the temperature to be measured as closely as possible to the spinning rotor. The entire top assembly including the MAS stator is enclosed in a Teflon insulating cavity attached to the outer probe shield. In combination with an additional probe body purge air flow, this is sufficient to prevent condensation from forming on the probe down to −150 °C. VT gas exits the stator, mixes with room temperature drive and bearing air, and is then expelled through a hole in the top of the insulating cavity.

Cooling below −20 °C is achieved using a commercial liquid nitrogen-cooled heat exchanger (Varian NMR), which is depicted in Fig. 2A. The VT gas cools on passing through a coil immersed in liquid nitrogen. This travels to the glass dewar at the bottom of the probe through a flexible vacuum jacketed stainless transfer line. This line is attached to the probe by an aluminum adapter clamp, insulated on the inside with polyethylene foam. This arrangement provides an efficiently insulated and mechanically robust delivery path for the VT gas to the stator. The transfer line remains flexible at all temperatures, thereby making it possible to move the probe up and down for exchange of samples while cold. Condensation of gas in the heat exchanger coil is prevented by pressurizing the liquid nitrogen reservoir, which raises the temperature of the liquid nitrogen bath. Room temperature purge air blows over the electronic components during VT use. Use of the purge gas prevents tuning drift due to shrinkage in the Teflon dielectric pieces of the probe's coaxial capacitors. The air temperature near the sample is controlled by regulating the flow of room temperature nitrogen gas through the heat exchanger. Addition of an inline heater with feedback control would be straightforward, but was not found to be required. This device works well over the range −140 to −20 °C. Below this range liquid nitrogen intermittently splashes onto the sample coil causing tuning instability. Above this range the flow of nitrogen gas through the heat exchanger is very low and difficult to control reproducibly.
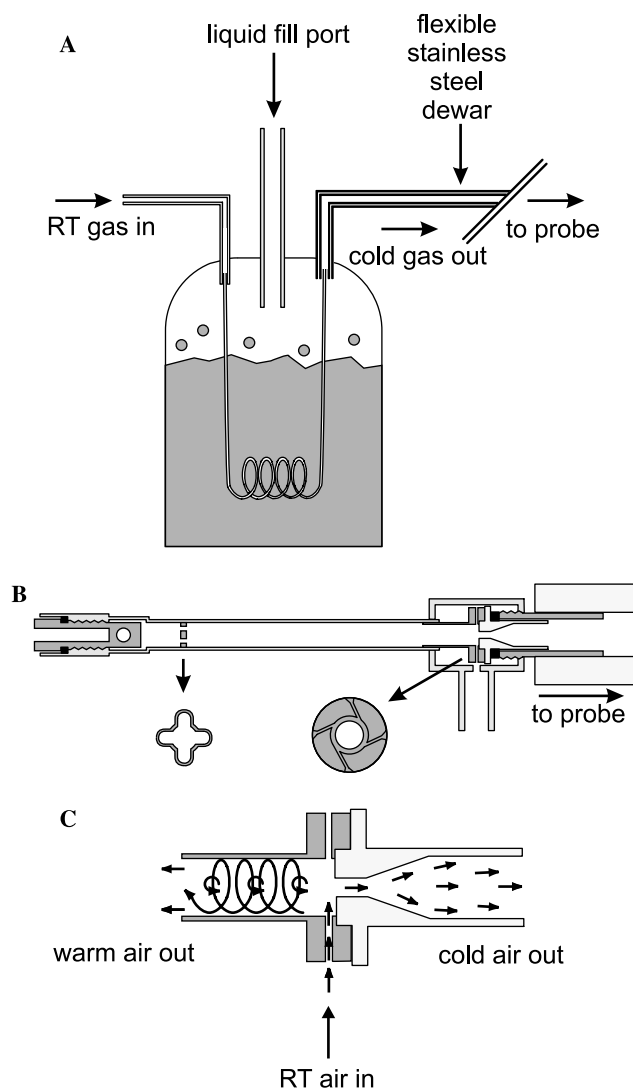

Fig. 2. (A) Temperatures below −20 °C are achieved using a liquid nitrogen heat exchanger. Nitrogen gas is delivered from this apparatus to the probe via a flexible stainless steel dewared transfer line as shown. The nitrogen reservoir is pressurized to about 30 psig. (B) Temperatures down to −20 °C can be maintained using a vortex tube cooling device. A cross-section of the vortex tube is shown. The right inset shows the brass piece that is responsible for inducing rotation of the compressed air, forming a vortex. The left inset shows a barrier placed in the warm end of the tube to partition the air flow. (C) Schematic depiction of the air flow within the vortex tube. Compressed air at room temperature enters the device producing a rotating vortex that is separated into a warm stream to the left, and a cold stream that is diverted to an expanding nozzle to the right.

Above −20 °C a commercially available vortex tube is used to provide the cooling air (Exair, model 3204, Ohio, or ITW Vortec, model 106-4-H, Ohio). The vortex tube is connected to the probe via a plastic adapter that makes its output end the same diameter as the flexible stainless steel dewared transfer line of the liquid nitrogen-cooled heat exchanger. The vortex tube was first described by Ranque [12] and was later described in

greater detail by Hilsch [13]. This device takes an input of pressurized, room temperature air and produces a stream of warm air and a stream of cold air. Vortex-tube cooling has been used in applications ranging from cooling parts being machined to temperature control in a sample cell for infrared spectroscopy [16].

A schematic of a Ranque–Hilsch vortex tube is shown in Fig. 2B. Air enters through a small hole in the side of the tube, tangent to the outer wall. Upon entering the device, the compressed air is forced through a brass piece with asymmetric air channels (right inset). The shape of these air passages induces rotation of the high-pressure air, creating a vortex. Hot air swirls around the tube walls, while cold air returns through the center of the hot air stream, as depicted in Fig. 2C. The geometry of the valve located at the hot end of the tube is optimized for releasing the warmest air and reflecting the cooler center stream. A small orifice on the cold side permits the air from the center stream to exit while the warm air from the sides of the tube is ejected at the opposite end. The temperature at the cool end of the tube can be regulated by adjusting the valve located at the hot end. The exact method by which the temperature separation is generated is not yet quantitatively understood, and is the subject of ongoing research [17,18]. According to the analysis of Hilsch, the cooling effect is generated by decompression and expansion of the gas in the center stream, while the heating of the outer layers is due to friction. Although this device is sometimes compared to "Maxwell's Demon," it should be noted that the pressure of the air leaving the tube is significantly less than the input pressure, with the compressed air providing the work needed to obtain the temperature separation.

With sufficient input pressure, it is possible to attain temperatures 40 °C above and below the temperature of the input stream [19]. In our application the cooling achieved by the vortex tube is limited by back pressure produced by the small inner diameter of the glass dewar at the cold end. This results in less efficient cooling than would be possible with free flow from the tube. In our laboratory the vortex tube is used to provide temperatures down to −20 °C, given an input temperature of approximately 22 °C and an input pressure of 100 psig supplied by the house air. If lower temperatures are not required, more efficient sample cooling is possible by directly connecting the vortex tube to the MAS stator. One may also conveniently cool the gas supply to the air bearings using additional inline vortex coolers. In this instance the high-pressure applied to the inline vortex cooler is supplied by the usual regulators used to control the MAS air bearing pressure. A separate small diameter airline is then also attached on the downstream cold side to make it possible to monitor the actual resulting air pressure that is applied to the MAS spinner air bearings.

4. Gallium arsenide optical thermometer and sensor magnetic field compensation

The fiber optic temperature sensor used in the probe (Nortech Fibronics/FISO Technologies, model Reflex TS-RX1-FL-0-10, Quebec) capitalizes on the temperature dependence of the optical absorption band edge of gallium arsenide (GaAs), which follows the temperature dependence of the semiconductor band gap (E_{gap}) according to the following empirical relation [20]:

$$E_{gap} = 1.522 - \frac{5.8 \times 10^{-4} T^2}{T + 300} \, (\text{eV}). \tag{1}$$

A least squares fit of this function to a straight line over the temperature range 240–310 K used in our calibration gives a regression line relating the temperature T (K) to the band gap:

$$T = -2370 E_{gap} + 3702.1 \tag{2}$$

with $R^2 = 0.9999$. The Nortech fiber optic thermometer is a simple optical spectrometer that measures the position of the absorption edge by reflectance, followed by a conversion of this wavelength measurement to a temperature reading via firmware. The conversion is made using an empirical equation similar to the one quoted above, but including correction factors for the particular sample of GaAs used as the sensor. These additional correction factors are required because the band gap of GaAs is also affected by the concentration of impurities [21].

E_{gap} is also expected to have a weak dependence on magnetic field strength (B_0) and on the orientation of the GaAs crystal in the magnetic field. The magnetic field dependence of the absorption spectrum has been exploited in the characterization of GaAs quantum wells. This dependence has been reported for both quantum wells and bulk GaAs [22]. A theoretical model predicting both linear and quadratic components to the field dependence shows sufficient agreement with these data [23]. Since the magnetic field dependence is weak, we assume it provides an additive contribution to the temperature dependence. At a given temperature, the band gap is expected to have the following form:

$$E_{gap}(B_0, T) = E_{gap, B_0=0}(T) + \alpha B_0 + \beta B_0^2, \tag{3}$$

where α and β are temperature independent empirical constants characteristic of the GaAs sample. If the band gap is used to measure the temperature without correction for the magnetic field dependence, the apparent temperature will be:

$$\begin{aligned} T_{apparent} &= -2370.7 \cdot E_{gap, B_0=0}(T) + 3702.1 \\ &= T - 2370.7(\alpha B_0 + \beta B_0^2). \end{aligned} \tag{4}$$

Assuming that the temperature dependence of the GaAs band gap has the same slope as quoted above in the temperature range at which our measurements were

made, there should be a field dependent temperature offset $\Delta T = T_{apparent} - T$ between the apparent temperature $T_{apparent}$ and the actual temperature T. Since the band gap increases with magnetic field, ΔT is predicted to be negative (as is observed).

5. Cross-calibration with the methanol NMR thermometer

To characterize the field dependence of the GaAs based fiber optic thermometer used in this probe, the apparent temperature was calibrated relative to the methanol chemical shift thermometer at five different field strengths using standard solution NMR probes. At each field strength, the temperature was measured simultaneously with the fiber optic thermometer (to $\pm 0.1\,^{\circ}C$) and using the chemical shift difference between the methyl and hydroxyl protons in methanol [24]. The methanol sample was dried over calcium hydride and sealed in a 5 mm NMR tube capped with a rubber septum. The fiber optic probe was inserted through a small hole in the septum such that the temperature sensor was immersed in the methanol. The temperature sensor was also coated with Halocarbon 1500 wax in order to prevent possible chemical interaction with the methanol. The experimental apparatus used for the temperature calibrations is shown in Fig. 3. The temperature was measured over the range of -25 to $25\,^{\circ}C$ in $5\,^{\circ}$ intervals. Data points were taken 20 min apart to allow the temperature to equilibrate. At each magnetic field point, the apparent temperature as measured by the fiber optic sensor was fit to a linear function of the temperature measured using the methanol thermometer, which is taken as the actual temperature of the sample.

$$T_{apparent} = aT_{MeOH} + b. \tag{5}$$

The numbers presented for the 500 and 800 MHz spectrometers are the result of averaging the data for two experimental trials on each instrument. The results of these experiments are shown in Table 1.

In all cases the correlation between the two thermometry methods is linear. The slopes are in general close to unity as expected. These observations support the notion that the field-induced error is an approximately fixed offset for a given B_0, therefore the ΔT values at each field strength were averaged. This field dependent offset is expected to vary as $\Delta T = -2370.7(\alpha B_0 + \beta B_0^2)$. A fit to this expected functional form is shown in Fig. 4. The best fit gives the correction factors as $\alpha = 1.32 \times 10^{-5}$ eV/Tesla and $\beta = 1.08 \times 10^{-4}$ eV/Tesla^2, with an R^2 value of 0.9929.
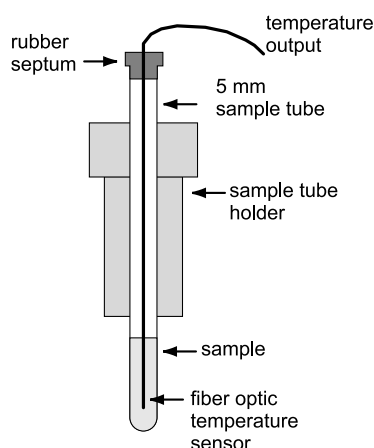

Fig. 3. The experimental apparatus used in calibration of the fiber optic thermometer relative to the methanol chemical shift thermometer. The fiber optic was introduced through a rubber septum capping the 5 mm NMR tube containing dry methanol.
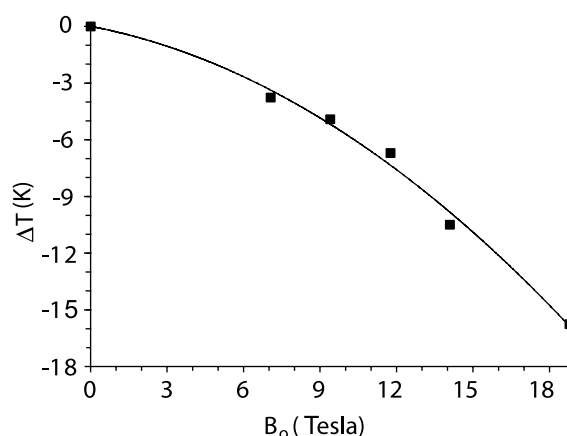

Fig. 4. A plot of the field dependent temperature offset ΔT for the GaAs fiber optic thermometer. The dependence is quadratic as expected.

Table 1
Calibration results for GaAs fiber optic thermometer

^1H frequency (MHz)	B (Tesla)	b (K)	$a = \frac{dT_{apparent}}{dT_{MeOH}}$	R^2	Average ΔT (K)
300.513	7.058	−3.7	0.99	0.9984	−3.8
399.998	9.395	−5.1	0.95	0.9979	−4.9
500.593	11.757	−6.7	0.96	0.9952	−6.7
599.859	14.089	−10.5	1.00	0.9989	−10.5
799.747	18.784	−15.8	1.02	0.9989	−15.7

A systematic error not accounted for here is the expected orientation dependence of the band gap with respect to the magnetic field. Since our analysis is intended to only identify the nature and source of the field dependent temperature error in this type of thermometer, no attempt was made to investigate this aspect of the temperature shift. This dependence is assumed to be small, and as the position of the GaAs sample is fixed in this application, this effect is likely to be implicitly included in the calibration.

6. Summary

Fast MAS combined with strong decoupling power can cause significant sample heating which in turn may cause degradation or denaturation in biological samples. It is found that the Q-loading induced by hydrated protein samples of moderate salt concentration can be characterized by the frequency shift of the probe resonance frequency. This shift, and the indicated loading of the probe, are functions of the sample temperature. Cooling of a nanocrystalline ubiquitin sample to a temperature corresponding to its glass transition is found to suppress loading of the probe Q, presumably by freezing out the molecular motions that give rise to the loss mechanism in the first place. The relative roles of conductive and dielectric losses in RF heating of protein crystals in high field MAS probes remains an open issue for investigation, as does a quantitative model for how any measure of this loss translates into a specific level of sample heating.

Until the development of a convenient internal NMR thermometer, this problem is most directly handled by cooling the air around the sample and closely monitoring the temperature close to the sample. The convenient approach to variable temperature operation described here uses the combination of a vortex cooler for cooling and a fiber optic temperature sensor for temperature measurement. The particular probe described here is capable of operating at −140 °C for several days with a liquid nitrogen cooled heat exchanger, and can continuously operate at −20 °C with the vortex tube cooler. Temperature measurement with a GaAs fiber optic thermometer has the advantage of being free of interference with the RF electronics. Such sensors have a well-defined magnetic field dependence that we have characterized here. The same approach using cross-validation with the standard methanol NMR thermometer can be applied to other types of fiber-optic temperature sensors as well.

References

[1] A. Bielecki, D.P. Burum, Temperature-dependence of Pb-207 MAS spectra of solid lead nitrate—an accurate, sensitive thermometer for variable-temperature MAS, J. Magn. Reson. Ser. A 116 (1995) 215–220.

[2] G. Neue, C. Dybowski, Determining temperature in a magic-angle spinning probe using the temperature dependence of the isotropic chemical shift of lead nitrate, Solid State Nucl. Magn. Reson. 7 (1997) 333–336.

[3] L.C.M. Vangorkom, J.M. Hook, M.B. Logan, J.V. Hanna, R.E. Wasylishen, Solid-state Pb-207 NMR of lead(II) nitrate—localized heating effects at high magic-angle-spinning speeds, Magn. Reson. Chem. 33 (1995) 791–795.

[4] B. Langer, L. Schnell, H.W. Spiess, A.R. Grimmer, Temperature calibration under ultrafast MAS conditions, J. Magn. Reson. 138 (1999) 182–186.

[5] F.D. Doty, P.D. Ellis, Design of high speed cylindrical NMR sample spinners, Rev. Sci. Instrum. 52 (1981) 1868–1875.

[6] J.J. Led, S.B. Petersen, Heating effects in carbon-13 NMR spectroscopy on aqueous solutions caused by proton noise decoupling at high frequencies, J. Magn. Reson. 32 (1978) 1–17.

[7] D.I. Hoult, P.C. Lauterbur, The sensitivity of the zeugmatographic experiment involving human samples, J. Magn. Reson. 34 (1979) 425–433.

[8] P.F. Flynn, D.L. Mattiello, H.D.W. Hill, A.J. Wand, Optimal use of cryogenic probe technology in NMR studies of proteins, J. Am. Chem. Soc. 122 (2000) 4823–4824.

[9] R.W. Dykstra, A technique to increase NMR sensitivity for conductive solutions, J. Magn. Reson. 84 (1989) 388–391.

[10] D.S. McNair, Heat-transfer in NMR of conductive samples with radiofrequency decoupling, J. Magn. Reson. 45 (1981) 490–502.

[11] D.W. Alderman, D.M. Grant, An efficient decoupler coil design which reduces heating in conductive samples in superconducting spectrometers, J. Magn. Reson. 36 (1979) 447–451.

[12] G.H. Ranque, Experiences sur la detente giratoire avec production simultanees d'un enchappement d'air chaud et d'air froid, J. Phys. Radium IV (1933) 112–114.

[13] R. Hilsch, Die Expansion von Gasen im Zentrifugalfeld als Kälteprozeβ, Z. Naturforsch. 1 (1946) 208–214.

[14] R.W. Martin, E.K. Paulson, K.W. Zilm, Design of a triple resonance magic angle spinning probe for high field solid state nuclear magnetic resonance, Rev. Sci. Instrum. 74 (2003) 3045–3061.

[15] R.W. Martin, K.W. Zilm, Preparation of protein nanocrystals and their characterization by solid-state NMR, J. Magn. Reson. 165 (2003) 162–174.

[16] T.J. Bruno, A simple and efficient low-temperature sample cell for infrared spectrophotometry, Rev. Sci. Instrum. 63 (1992) 4459–4460.

[17] M.H. Saidi, M.R. Allaf Yazdi, Exergy model of a vortex tube system with experimental results, Energy 24 (1999) 625–632.

[18] B.K. Ahlborn, J.M. Gordon, The vortex tube as a classic thermodynamic refrigeration cycle, J. Appl. Phys. 88 (2000) 3645.

[19] B. Ahlborn, J.U. Keller, R. Staudt, G. Treitz, E. Rebhan, Limits of temperature separation in a vortex tube, J. Phys. D: Appl. Phys. 27 (1994) 480–488.

[20] O. Madelung, W. vonder Osten, U. Rossler, Subvolume A: Intrinsic properties of group IV elements and IV–V, II–VI, and I–VII compounds, in: O. Madelung, M. Schulz (Eds.), Numerical

Data and Functional Relationships in Science and Technology, Group III, vol. 22, Springer-Verlag, Berlin, 1996, pp. 82–94.

[21] J. Silva-Valencia, N. Porras-Montenegro, Impurity-related optical-absorption spectra in GaAs-Ga$_{1-x}$ Al$_x$As superlattices with an in-plane magnetic field, Phys. Rev. B 58 (1998) 2094–2101.

[22] W.M. Zhou, D.D. Smith, H. Shen, J. Pamulapati, M. Dutta, A. Chin, J. Ballingall, Comparison of (111)-Grown and (001)-Grown GaAs-Al$_x$ Ga$_{1-x}$As Quantum-Wells by magnetoreflectance, Phys. Rev. B 45 (1992) 12156–12159.

[23] G. Duggan, Theory of heavy-hole magnetoexcitons in GaAs-(Al,Ga)As Quantum-Well heterostructures, Phys. Rev. B 37 (1988) 2759–2762.

[24] A.L. Van Geet, Calibration of methanol nuclear magnetic resonance thermometer at low temperature, Anal. Chem. 42 (1970) 679–680.